AFRL-AFOSR-VA-TR-2024-0098

DEFECT EQUILIBRATION STUDIES IN BINARY METAL-OXIDES

Shriram Ramanathan
PURDUE UNIVERSITY
2550 NORTHWESTERN AVE # 1100
WEST LAFAYETTE, IN, 47906
USA

01/14/2024
Final Technical Report

DISTRIBUTION A: Distribution approved for public release.

Air Force Research Laboratory
Air Force Office of Scientific Research
Arlington, Virginia 22203
Air Force Materiel Command

REPORT DOCUMENTATION PAGE

PLEASE DO NOT RETURN YOUR FORM TO THE ABOVE ORGANIZATION.

1. REPORT DATE 20240114	**2. REPORT TYPE** Final	**3. DATES COVERED** **START DATE** 20180515	**END DATE** 20220514

4. TITLE AND SUBTITLE
DEFECT EQUILIBRATION STUDIES IN BINARY METAL-OXIDES

5a. CONTRACT NUMBER	**5b. GRANT NUMBER** FA9550-18-1-0250	**5c. PROGRAM ELEMENT NUMBER** 61102F
5d. PROJECT NUMBER	**5e. TASK NUMBER**	**5f. WORK UNIT NUMBER**

6. AUTHOR(S)
Shriram Ramanathan

7. PERFORMING ORGANIZATION NAME(S) AND ADDRESS(ES)
PURDUE UNIVERSITY
2550 NORTHWESTERN AVE # 1100
WEST LAFAYETTE, IN 47906
USA

8. PERFORMING ORGANIZATION REPORT NUMBER

9. SPONSORING/MONITORING AGENCY NAME(S) AND ADDRESS(ES)
Air Force Office of Scientific Research
875 N. Randolph St. Room 3112
Arlington, VA 22203

10. SPONSOR/MONITOR'S ACRONYM(S)
AFRL/AFOSR RTB1

11. SPONSOR/MONITOR'S REPORT NUMBER(S)
AFRL-AFOSR-VA-TR-2024-0098

12. DISTRIBUTION/AVAILABILITY STATEMENT
A Distribution Unlimited: PB Public Release

13. SUPPLEMENTARY NOTES

14. ABSTRACT
The project goals include creation of extreme environments such as oxygen concentration gradients; exposure to strong optical and electric fields to synthesize and modulate physical properties of oxide materials focusing on defect equilibration. Using model systems such as VO2, NiO that show collective response to structural and defect density changes, we can both study the microstructural aspects from a fundamental point of view, charge compensation mechanisms including use of X-ray spectroscopy and further explore the use of metastable phases in emerging fields. In this final report, we discuss representative studies on VO2 and NiO thin films that undergoes a structural and electronic phase changes under strong fields.

15. SUBJECT TERMS

16. SECURITY CLASSIFICATION OF:			**17. LIMITATION OF ABSTRACT**	**18. NUMBER OF PAGES**
a. REPORT U	**b. ABSTRACT** U	**c. THIS PAGE** U	UU	9

19a. NAME OF RESPONSIBLE PERSON
ALI SAYIR

19b. PHONE NUMBER *(Include area code)*
426-7236

Standard Form 298 (Rev.5/2020)
Prescribed by ANSI Std. Z39.18

Award Number: FA9550-18-1-0250

Report type: Final

Reporting period: 05/2018-05/2022

Distribution statement: Approved for public release

Program Officer Name: Dr. Ali Sayir

PI name: Shriram Ramanathan

Project title: Defect equilibration studies in binary metal oxide films

Abstract

The project goals include creation of extreme environments such as oxygen concentration gradients; exposure to strong optical and electric fields to synthesize and modulate physical properties of oxide materials focusing on defect equilibration. Using model systems such as VO_2, NiO that show collective response to structural and defect density changes, we can both study the microstructural aspects from a fundamental point of view, charge compensation mechanisms including use of X-ray spectroscopy and further explore the use of metastable phases in emerging fields. In this final report, we discuss representative studies on VO_2 and NiO thin films that undergoes a structural and electronic phase changes under strong fields.

Phase transition in VO_2 and response to optical fields

Vanadium dioxide undergoes insulator-metal transition near room temperature when driven by external fields such as temperature, electrical and/or optical stimuli. Understanding the interplay between structural and electrical phase evolution is an important scientific theme, and in addition the resulting changes in physical properties find interesting use in several areas. Here, we report a model example of growth of VO_2 onto GaAs substrates followed by their response to laser illumination as optical limiter. The optical measurements and modeling were performed by collaborators at the University of Wisconsin (Professor M. A. Kats group) and briefly discussed here.

VO_2 was deposited onto double-side-polished undoped GaAs (001) wafers via magnetron sputtering from a V_2O_5 target, with radio-frequency power of 100 W. During deposition, the chamber pressure was maintained at 5 mTorr with an Ar/O_2 gas mixture at a flow rate of 49.85/0.15 sccm. The substrate was heated to 700 °C to form the VO_2 phase. A 50-nm gold FSS was fabricated on the as-grown VO_2. First, a ~250-nm PMMA (495 PMMA A4) was spin-coated onto the VO_2 film and the pattern was written using an e-beam lithography system. After development in MIBK/IPA, an array of cross-shape PMMA blocks were left on top of the VO_2. Then, 50 nm of gold was evaporated, and the sample was soaked in an acetone bath for a few minutes to lift off the gold-PMMA blocks, leaving an array of cross-slit apertures within the gold film. Figure 1 shows the characterization of the grown films. The thickness of the resulting film is ~105 nm, measured by scanning electron microscopy (SEM, Zeiss LEO 1530) imaging of the cross section, which is close to our target thickness (100 nm) that was used in optical simulation. Atomic force microscopy (AFM, Bruker MultiMode 8) imaging confirmed that the film was continuous with a surface roughness of $Ra \cong 6$ nm. The stoichiometry of the film was confirmed by Raman spectroscopy measurements at 30 °C and 100 °C, with the pump laser operating at 520 nm (Figure S3b). At 30 °C, signature Raman modes of insulator-phase VO_2 at 140, 192, 223, 308, 387, 395, 613, and 823 cm^{-1} were detected;[S5] while at 100 °C, the VO_2 is in the metallic state and only features of the GaAs substrate were observed. We did not find any clear Raman modes of V_2O_5 to confirm that there is a surface oxide on top of the as-grown VO_2 film. One plausible explanation is that such surface oxide may be too thin (and perhaps not continuous) to be identified by our Raman measurements.

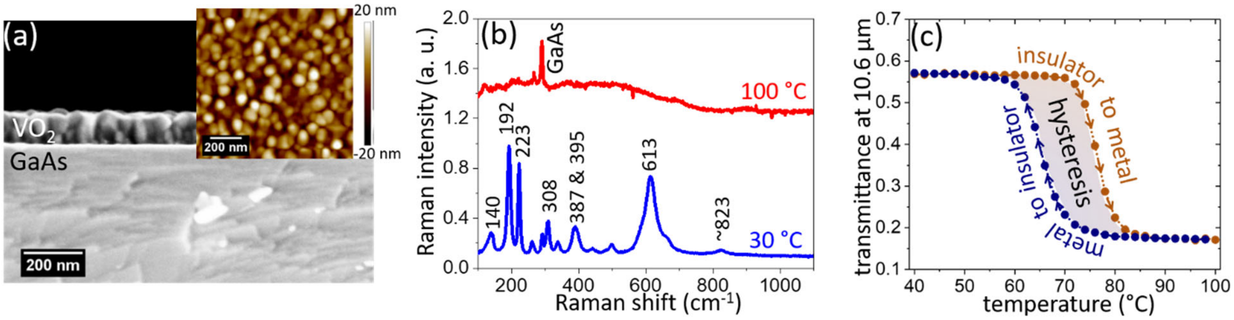

Figure 1. (a) Cross-section SEM of the VO_2 film on GaAs. The inset is AFM characterization of the film surface, indicating the film roughness of ~6 nm. **(b)** Raman spectra of the as-grown VO_2 at 30 and 100 °C. At 30 °C, signatures of insulator-phase VO_2 were identified, while at 100 °C only peaks of the GaAs

substrate were observed. **(c)** Temperature-dependent transmittance at λ = 10.6 μm, measured under heating (brown) and cooling (blue).

As example of representative functional property measurements, figure 2 details the fabrication process and optical measurements reported with the VO_2 film by Professor Kats group. The as-grown VO_2 film features broadband transmittance of ~0.6 in the insulating phase and relatively low transmittance when thermally biased to the metallic phase (Figure 2c). The absorptance spectrum at 100 °C (absorptance = 1 – transmittance – reflectance) indicates that the metallic-state VO_2 has a relatively high absorptance of ~0.3 at all wavelengths. A 50-nm gold FSS was built on top of the as-grown VO_2 via steps as shown in Figure 2a. At 30 °C the FSS-VO_2 limiter displays a peak transmittance of 0.45 at λ = 9.8 μm, while the transmittance decreased to ~0.03 when the temperature was increased to 100 °C (Figure 2d). The measured reflectance in the limiting state is >0.9 at all wavelengths (Figure 2f), indicating that the limiting-state absorptance is <0.06 (Figure 2d), which is substantially reduced compared to that of the bare VO_2 film. Further we fabricated samples with different aperture lengths. The measurements (Figure 2g) showed that limiters with different aperture lengths (d_1 = 1, 1.5, 2, 2.5, and 3 μm) have central wavelengths of resonant transmittance ranging from 4 to 11 μm, as expected based on the simulations in Figure 1d. The IMT in VO_2 can be a source of giant photothermal nonlinearity, which could be useful to explore in future particularly combining electrical and optical fields to tune the threshold for onset of non-linear properties.

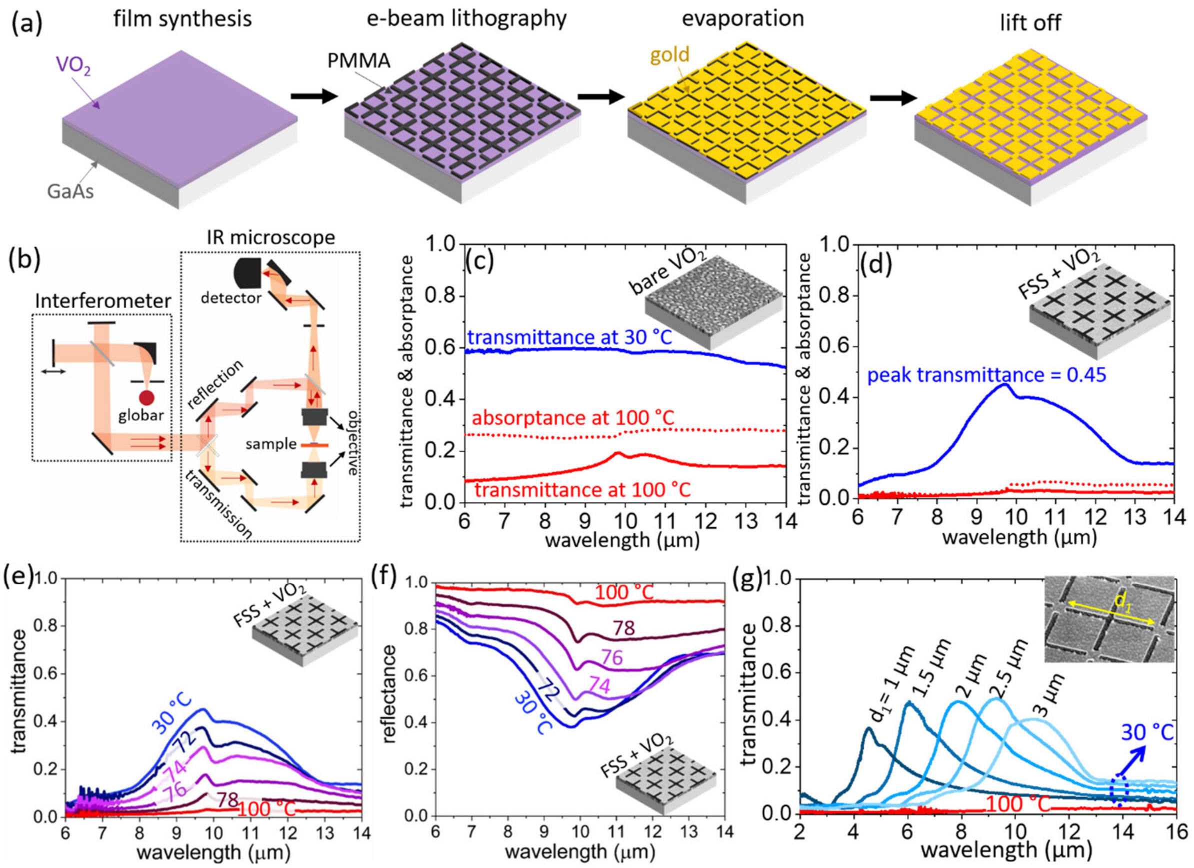

Figure 2. **(a)** 100-nm VO_2 on GaAs wafer was deposited using magnetron sputtering. The as-grown film went through an e-beam lithography and development, resulting in an array of cross-shape blocks of PMMA. Then, we evaporated 50 nm of gold on top, and performed a lift-off process, leaving an array of cross-slit apertures. **(b)** Schematic of optical path of Kats group FTIR transmission and reflection measurements. **(c)** Transmittance and absorptance spectra of the as-grown VO_2 film, for insulating (30 °C) and metallic (100 °C) phases. **(d)** Transmittance and absorptance spectra of the FSS-VO_2 limiter at 30 °C (open state) and 100 °C (limiting state). **(e, f)** Transmittance and reflectance measurements of FSS-VO_2 limiter when VO_2 in its pure insulating phase (30 °C), pure metallic phase (100 °C), and intermediate phases across the IMT (at 72, 74, 76, and 78 °C). **(g)** Measured transmittance of the FSS-VO_2 limiters with aperture lengths d_1 of 1, 1.5, 2, 2.5, and 3 µm, for both open (30 °C) and limiting (100 °C) states.

Relaxation dynamics of NiO to oxygen chemical potential changes

The response of NiO to dynamic environmental stimulus was studied using a home-built *in-situ* testing chamber with switchable gases. Schematic illustration of the chamber is shown in Fig. 3(a) where NiO thin films were placed in a sealed temperature-controlled probe station. Extreme reducing and oxidizing environment with $p(O_2)$ spanning several orders of magnitudes was generated by 5% Argon balanced H_2 gas and O_3 gases. The gas flow was kept as 100 ml/min to enable a steep switch of chamber environment [Fig. 3(b)]. It takes about two seconds for the chamber to reach equilibrium after switching which allows us to study the intrinsic response of NiO in different environments. NiO thin films with thickness of ~ 100 nm was deposited on sapphire substrate by magnetron sputtering of pure Ni target. To measure the electrical properties, parallel platinum electrodes with thickness of 100 nm were deposited on top of NiO thin films using shadow mask by electron beam evaporation.

Figure 3(c) shows the relative resistance modulation of NiO at 200 ºC with 15 min of H_2 exposure and relatively long time of H_2 withdrawal as 15 min. The NiO demonstrates a reversible behavior upon repeating of the H_2 exposure and complete forgetting of previous cyclic exposures due to the long-time interval in training which serves as control studies. With reducing the H_2 OFF time while maintain an identical H_2 ON time of 15 min, the response of NiO decreases monotonically [Fig. 3(d)], indicating habituation learning of H_2 stimulus. When a short exposure to O_3 for 15 s was introduced in between the habituation training cycles [Fig. 3(d)], a substantially increased response appears. The O_3 not only causes dishabituation but also results in an increase of response by ~ 10 times higher than that of pristine state, demonstrating a sensitization behavior of O_3 stimulus. The habituation and sensitization behavior of NiO can also be observed in extracted relaxation time during the training process [Fig. 3(e)], where the relaxation time monotonically decreases accompanying with habituation and sharply enlarges during sensitization. In addition, it is found that the relaxation time of NiO increases substantially with increasing electrical conductivity under environmental stimuli [Fig. 3(f)]. This clearly indicates that defect incorporation plays an important role in tuning both static properties (e.g. electrical resistance) and the kinetic behavior under changing environments.

The habituation and sensitization learning behavior of NiO can also be demonstrated at room temperature by utilizing UV light. Schematic of experimental setup is shown in Fig. 3(g), where a UV light source with an output wavelength spectrum from $\lambda = 185$ to 579 nm was placed on top of NiO device from a distance of 3 cm. The UV light breaks the environmental O_2 to forms O_3 [3], which then sensitizes the devices. The response of NiO in cyclic H_2 exposures and UV stimulus is shown in Fig. 3(h). With H_2 exposure of ~ 15 min in an interval of H_2 withdrawal ~ 15 min, NiO shows weak habituation behavior as slight decrease of response upon successive H_2 exposures. With introducing of UV stimulus ~ 5 min, the response of NiO is enhanced by ~ 6 times. Moreover, long term sensitization is observed in the following H_2 exposures. It therefore indicates the generality of sensitization behavior under multiple types of stimuli.

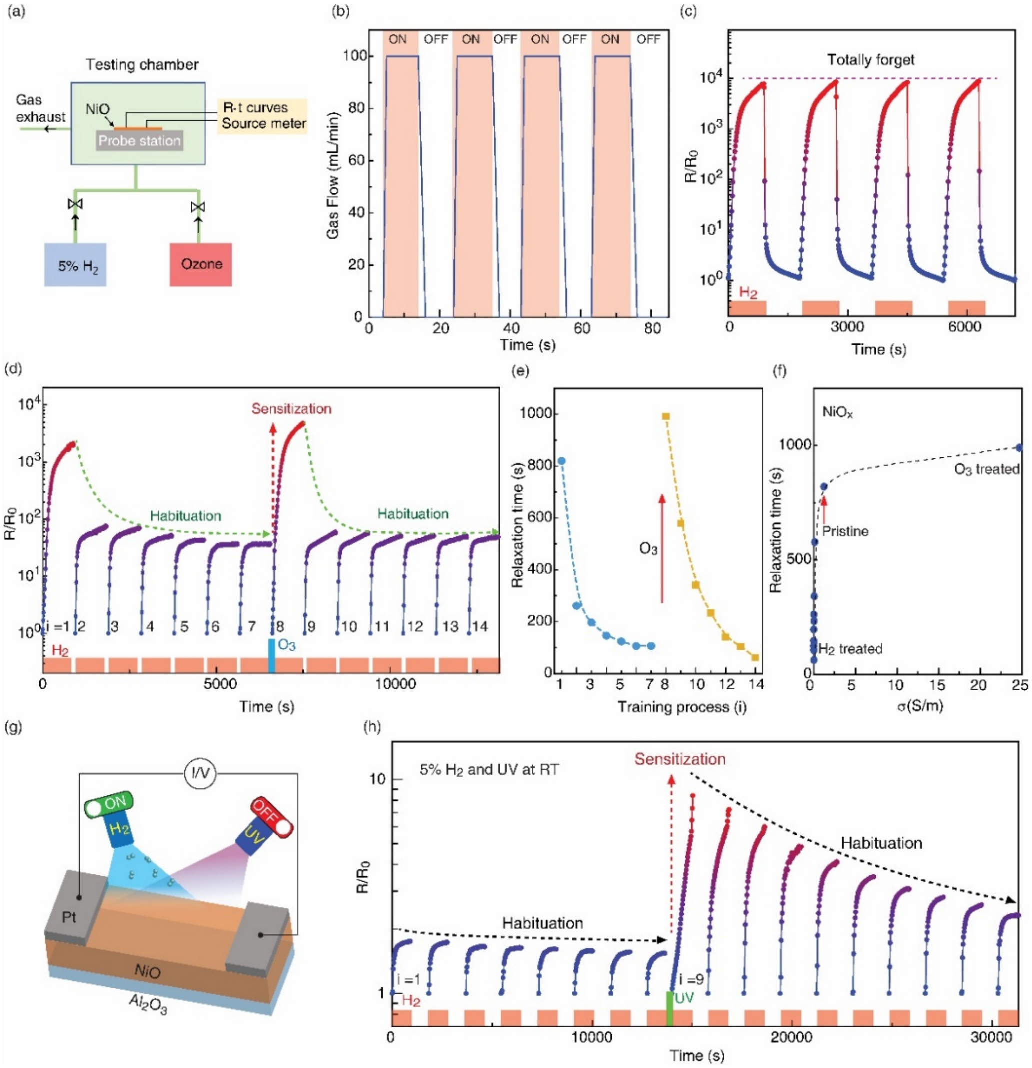

Figure 3. (a) Experimental setup on *in-situ* electrical measurement of NiO upon environmental stimuli. The chamber environment can be switched between 5% Argon balanced H_2 gas and O_3 gas. **(b)** Monitored gas flow of testing chamber as a function of time during switching H_2 gas ON and OFF. **(c)** Relative resistance modulation of NiO under successive H_2 exposures at 200 °C. Both H_2 ON and OFF time are 15 min. Reversibility and nearly identical response are observed. **(d)** Relative resistance modulation of NiO under repeating H_2 exposures and one time of O_3 exposure. The H_2 ON and OFF time are 15 min and 45s respectively. The duration of O_3 is 15s. With reducing H_2 withdrawal time here, the response of NiO decreases continuously, demonstrating a habituation learning behavior. After the O_3 exposure, the response of NiO becomes ever larger than pristine sample, indicating a sensitization behavior. **(e)** Relaxation time extracted from (d) as a function of training process. **(f)** Relaxation time as a function of electrical conductivity of NiO under defect incorporation. **(g)** Experimental setup on measuring the habituation and sensitization behavior of NiO at room temperature with UV light as sensitizer. **(h)** Relative resistance modulation of NiO under repeating H_2 exposures and UV stimulus. The H_2 ON and OFF time are both 15 min. The UV exposure time is 5 min. Long term sensitization behavior appears after UV exposure.

Mechanism on evolution of NiO under various environmental stimuli

To understand the evolution of electrical properties under environmental stimuli, systematic investigations on structure, defect state, and electronic structure of NiO were conducted. Figure 4(a) shows that the NiO is stable in air at 200 °C. By introducing 5% H_2 gas, the resistivity increases gradually by ~ four orders of magnitude; while the resistivity of sample drops by ~ two orders of magnitude during O_3 exposure, which indicates the metastability of NiO in H_2 and O_3 environment during the sensitization and habituation processes. We then quenched the metastable H_2 and O_3 exposed NiO to room temperature for further studies.

The structure evolution after the gas exposures was studied using X-ray diffraction and shown in Figs. 4(b) and (c). In wide 2θ range, the out-of-plane orientation of NiO with respect to sapphire substrate is intact and no new diffraction peak are observed, indicating the absence of secondary phase and structural degradation upon exposing in various gases. A narrow range scan around NiO (111) diffraction peaks shows a systematic shift which corresponding to out-of-plane lattice change of ~0.27%. X-ray photoemission spectra were utilized to study the evolution on defect state of NiO after gas exposures. The O 1s photoemission spectra of NiO is shown in Fig. 4(d) and fitted with photoemission from lattice oxygen at ~529.3 eV (O_L), oxygen defects (O_D, ~530.7 eV), and hydroxide group at ~ 531.7 eV (-OH). Under H_2 exposure, a predominance of -OH group peak appears indicating the incorporation of hydrogen into the lattice from the Pt triple phase boundary. For O_3 exposed NiO, an enlargement of defect oxygen peak occurs indicating the introduction of excess oxygen ions. Taking the area ratio of lattice oxygen and oxygen defects, the composition of NiO in pristine and after O_3 exposure are estimated approximately to be $NiO_{1.19}$ and $NiO_{1.38}$ respectively.

To understand the electrical response under gas exposures, we further studied the Ni L as well as O K X-ray absorption spectra of NiO collaboratively at Argonne National Laboratory. After exposure to H_2 gas, the spectral weight of the lower energy component at both Ni L-2 and L-3 peaks [Fig. 4(e)] increase substantially. At the same time, a diminishing of pre-peak at ~532 eV is observed at O-K edge [Fig. 4(f)]. This indicates electron filling of Ni 3*d* – O 2*p* hybridized orbitals upon hydrogenation, which compensates the pre-existing hole state and leads to the increased electrical resistance in H_2. Upon the sensitizing stimulus O_3, the spectral weight transfers to the higher energy components at Ni L-2 and L-3 peaks [Fig. 4(e)]. Notably, a new pre-peak at O-K edge emerges at ~529 eV at the expense of the one near ~ 532 eV [Fig. 4(f)], which indicates an increase in density of hole states and explains the decrease of electrical resistance of NiO in O_3 gas.

The sensitization behavior was further characterized using *in-situ* XANES measurement [Figs. 4(g) to (i)]. Pristine and O_3-exposed NiO were sealed in an *in-situ* environmental cell [5] and heated up to 150 ºC. The XANES spectra at Ni K edge of NiO were continuously collected when H_2 gas was introduced. As shown in Figs. 4(h) and 4(i), the lower energy shifting of the Ni K absorption edge of O_3 exposed NiO, corresponding to decrease of Ni valence state upon hydrogenation, is much larger than that of pristine sample, which then confirms the sensitization behavior.

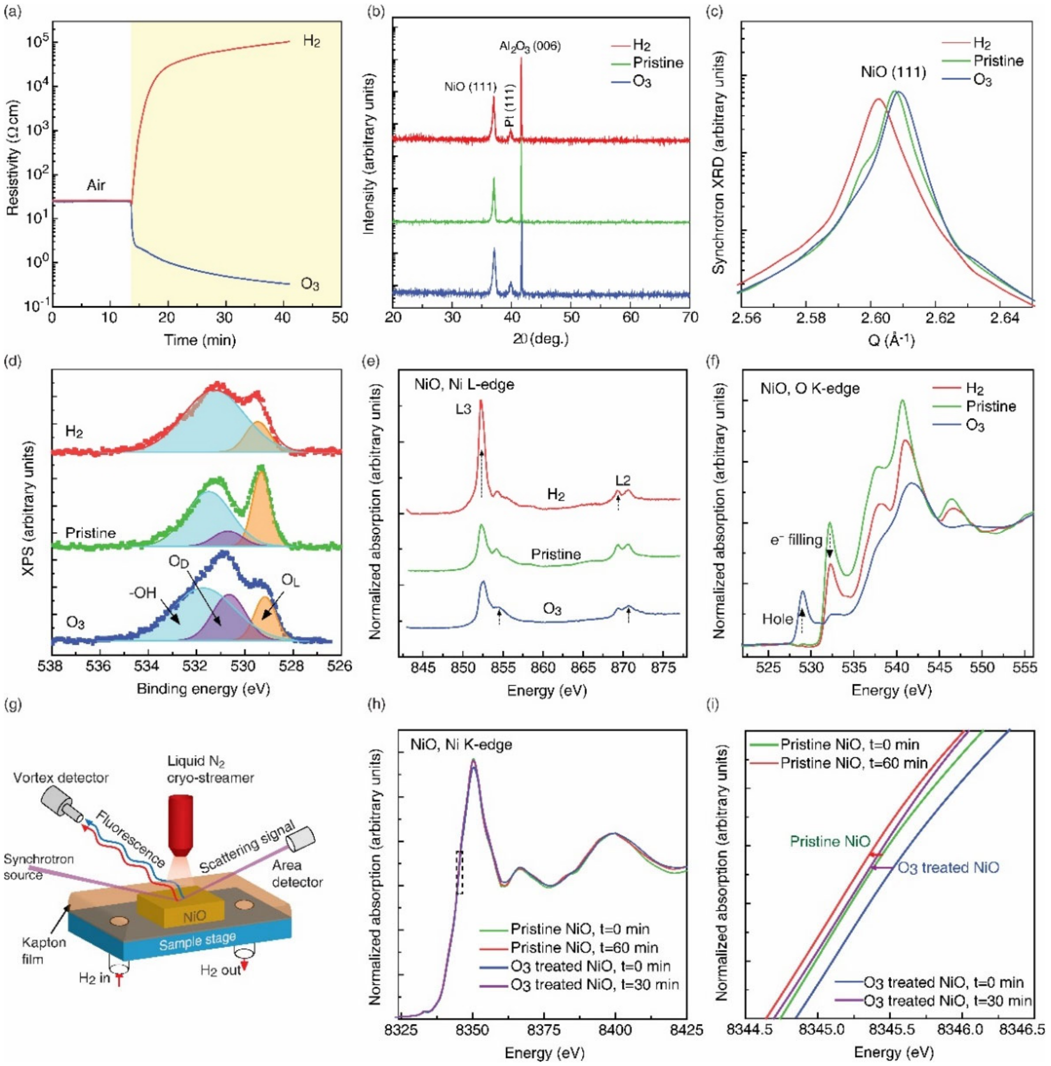

Figure 4. (a) *In-situ* resistivity – time results of NiO during exposure of 5% H_2 and O_3 respectively at 200 °C. Overall, more than five orders of magnitude resistivity modulation appear. **(b) and (c)** Room temperature X-ray diffraction profile after exposures in wide (b) and narrow (c) 2θ angle range. The out-of-plane lattice constant of NiO changes by 0.27% between H_2 and O_3 exposures. **(d)** O 1s X-ray photoemission spectra after exposures. The predominance of hydroxide group peak (-OH, blue color) in H_2 exposed NiO indicates the incorporation of hydrogen into the lattice, while the enlarged oxygen defect peak (O_D, purple color) indicates the accumulation of excess oxygen defects. **(e)** Normalized Ni L-edge X-ray absorption spectra of NiO after exposures. The shifting of spectrum weight indicates the variation of valence state of Ni under gas stimulus. **(f)** O K-edge X-ray absorption spectra of NiO after exposures. The pre-peak at O K-edge shifts its weight from ~532 eV to ~529 eV in O_3, which indicates the accumulation of hole state, corresponding to the resistivity decrease. **(g)** Schematic of *in-situ* XANES setup to monitor the response of NiO in H_2. **(h)** and **(i)** *In-situ* XANES spectra on Ni K-edge of pristine and O_3 treated NiO. The lower energy shift on absorption edge of O_3 treated NiO (~0.2 eV) is larger than that of pristine sample (~0.1 eV) after a shorter H_2 exposure period.

Summary: Exposure to extreme environments such as oxygen potential changes, optical fields can induce phase transformations in binary oxides such as VO2, NiO that have fragile electronic structures which can be perturbed in a dynamic and reversible manner. The charge compensation mechanisms enable experimental measurement of changes to electrical or optical properties. for instance in the case of NiO, we found that rapid fluctuations in the environment can result in gradual reduction in response due to non-equilibration of defects. In the case of vanadium dioxide, exposure to strong optical fields resulted in non-linear absorption characteristics that can be magnified near structural phase transition boundaries. In future, defect engineering of the structural phase boundaries can offer new routes to tune the temperature sensitivity.